Gravitational Test Beyond the First Post-Newtonian Order with the Shadow of the M87 Black Hole

Dimitrios Psaltis,[1] Lia Medeiros,[2] Pierre Christian,[1] Feryal Özel,[1] Kazunori Akiyama,[3,4,5,6] Antxon Alberdi,[7] Walter Alef,[8] Keiichi Asada,[9] Rebecca Azulay,[10,11,8] David Ball,[1] Mislav Baloković,[6,12] John Barrett,[4] Dan Bintley,[13] Lindy Blackburn,[6,12] Wilfred Boland,[14] Geoffrey C. Bower,[15] Michael Bremer,[16] Christiaan D. Brinkerink,[17] Roger Brissenden,[6,12] Silke Britzen,[8] Dominique Broguiere,[16] Thomas Bronzwaer,[17] Do-Young Byun,[18,19] John E. Carlstrom,[20,21,22,23] Andrew Chael,[24] Chi-kwan Chan,[1,25] Shami Chatterjee,[26] Koushik Chatterjee,[27] Ming-Tang Chen,[15] Yongjun Chen,[28,29] Ilje Cho,[18,19] John E. Conway,[30] James M. Cordes,[26] Geoffrey B. Crew,[4] Yuzhu Cui,[31,32] Jordy Davelaar,[17] Mariafelicia De Laurentis,[33,34,35] Roger Deane,[36,37] Jessica Dempsey,[13] Gregory Desvignes,[38] Jason Dexter,[39] Ralph P. Eatough,[8] Heino Falcke,[17] Vincent L. Fish,[4] Ed Fomalont,[3] Raquel Fraga-Encinas,[17] Per Friberg,[13] Christian M. Fromm,[34] Charles F. Gammie,[40,41] Roberto García,[16] Olivier Gentaz,[16] Ciriaco Goddi,[17,42] José L. Gómez,[7] Minfeng Gu,[28,43] Mark Gurwell,[12] Kazuhiro Hada,[31,32] Ronald Hesper,[44] Luis C. Ho,[45,46] Paul Ho,[9] Mareki Honma,[31,32,47] Chih-Wei L. Huang,[9] Lei Huang,[28,43] David H. Hughes,[48] Makoto Inoue,[9] Sara Issaoun,[17] David J. James,[6,12] Buell T. Jannuzi,[1] Michael Janssen,[17] Wu Jiang,[28] Alejandra Jimenez-Rosales,[49] Michael D. Johnson,[6,12] Svetlana Jorstad,[50,51] Taehyun Jung,[18,19] Mansour Karami,[52,53] Ramesh Karuppusamy,[8] Tomohisa Kawashima,[5] Garrett K. Keating,[12] Mark Kettenis,[54] Jae-Young Kim,[8] Junhan Kim,[1,55] Jongsoo Kim,[18] Motoki Kino,[5,56] Jun Yi Koay,[9] Patrick M. Koch,[9] Shoko Koyama,[9] Michael Kramer,[8] Carsten Kramer,[16] Thomas P. Krichbaum,[8] Cheng-Yu Kuo,[57] Tod R. Lauer,[58] Sang-Sung Lee,[18] Yan-Rong Li,[59] Zhiyuan Li,[60,61] Michael Lindqvist,[30] Rocco Lico,[7,8] Jun Liu,[62] Kuo Liu,[8] Elisabetta Liuzzo,[63] Wen-Ping Lo,[9,64] Andrei P. Lobanov,[8] Colin Lonsdale,[4] Ru-Sen Lu,[28,29,8] Jirong Mao,[65,66,67] Sera Markoff,[27,68] Daniel P. Marrone,[1] Alan P. Marscher,[50] Iván Martí-Vidal,[10,11] Satoki Matsushita,[9] Yosuke Mizuno,[34,69] Izumi Mizuno,[13] James M. Moran,[6,12] Kotaro Moriyama,[4,31] Monika Moscibrodzka,[17] Cornelia Müller,[8,17] Gibwa Musoke,[27,17] Alejandro Mus Mejías,[10,11] Hiroshi Nagai,[5,32] Neil M. Nagar,[70] Ramesh Narayan,[6,12] Gopal Narayanan,[71] Iniyan Natarajan,[37] Roberto Neri,[16] Aristeidis Noutsos,[8] Hiroki Okino,[31,47] Héctor Olivares,[34] Tomoaki Oyama,[31] Daniel C. M. Palumbo,[6,12] Jongho Park,[9] Nimesh Patel,[12] Ue-Li Pen,[52,72,73,74] Vincent Piétu,[16] Richard Plambeck,[75] Aleksandar PopStefanija,[71] Ben Prather,[40] Jorge A. Preciado-López,[52] Venkatessh Ramakrishnan,[70] Ramprasad Rao,[15] Mark G. Rawlings,[13] Alexander W. Raymond,[6,12] Bart Ripperda,[76,77] Freek Roelofs,[17] Alan Rogers,[4] Eduardo Ros,[8] Mel Rose,[1] Arash Roshanineshat,[1] Helge Rottmann,[8] Alan L. Roy,[8] Chet Ruszczyk,[4] Benjamin R. Ryan,[78,79] Kazi L. J. Rygl,[63] Salvador Sánchez,[80] David Sánchez-Arguelles,[48,81] Mahito Sasada,[31,82] Tuomas Savolainen,[83,84,8] F. Peter Schloerb,[71] Karl-Friedrich Schuster,[16] Lijing Shao,[8,46] Zhiqiang Shen,[28,29] Des Small,[54] Bong Won Sohn,[18,19,85] Jason SooHoo,[4] Fumie Tazaki,[31] Remo P. J. Tilanus,[17,42,86,1] Michael Titus,[4] Pablo Torne,[8,80] Tyler Trent,[1] Efthalia Traianou,[8] Sascha Trippe,[87] Ilse van Bemmel,[54] Huib Jan van Langevelde,[54,88] Daniel R. van Rossum,[17] Jan Wagner,[8] John Wardle,[89] Derek Ward-Thompson,[90] Jonathan Weintroub,[6,12] Norbert Wex,[8] Robert Wharton,[8] Maciek Wielgus,[6,12] George N. Wong,[40,78] Qingwen Wu,[91] Doosoo Yoon,[27] André Young,[17] Ken Young,[12] Ziri Younsi,[92,34] Feng Yuan,[28,43,93] Ye-Fei Yuan,[94] and Shan-Shan Zhao[17,60]

(the EHT Collaboration)

[1] *Steward Observatory and Department of Astronomy, University of Arizona, 933 N. Cherry Ave., Tucson, AZ 85721, USA*

[2] *School of Natural Sciences, Institute for Advanced Study, 1 Einstein Drive, Princeton, NJ 08540, USA*

[3] *National Radio Astronomy Observatory, 520 Edgemont Rd, Charlottesville, VA 22903, USA*

[4] *Massachusetts Institute of Technology Haystack Observatory, 99 Millstone Road, Westford, MA 01886, USA*

[5] *National Astronomical Observatory of Japan, 2-21-1 Osawa, Mitaka, Tokyo 181-8588, Japan*

[6] *Black Hole Initiative at Harvard University, 20 Garden Street, Cambridge, MA 02138, USA*

[7] *Instituto de Astrofísica de Andalucía-CSIC, Glorieta de la Astronomía s/n, E-18008 Granada, Spain*

[8] *Max-Planck-Institut für Radioastronomie, Auf dem Hügel 69, D-53121 Bonn, Germany*

[9] *Institute of Astronomy and Astrophysics, Academia Sinica, 11F of Astronomy-Mathematics Building, AS/NTU No. 1, Sec. 4, Roosevelt Rd, Taipei 10617, Taiwan, R.O.C.*

[10] *Departament d'Astronomia i Astrofísica, Universitat de València, C. Dr. Moliner 50, E-46100 Burjassot, València, Spain*

[11] *Observatori Astronòmic, Universitat de València, C. Catedrático José Beltrán 2, E-46980 Paterna, València, Spain*

[12] Center for Astrophysics — Harvard & Smithsonian, 60 Garden Street, Cambridge, MA 02138, USA
[13] East Asian Observatory, 660 N. A'ohoku Place, Hilo, HI 96720, USA
[14] Nederlandse Onderzoekschool voor Astronomie (NOVA),
PO Box 9513, 2300 RA Leiden, The Netherlands
[15] Institute of Astronomy and Astrophysics, Academia Sinica, 645 N. A'ohoku Place, Hilo, HI 96720, USA
[16] Institut de Radioastronomie Millimétrique, 300 rue de la Piscine, F-38406 Saint Martin d'Hères, France
[17] Department of Astrophysics, Institute for Mathematics,
Astrophysics and Particle Physics (IMAPP), Radboud University,
P.O. Box 9010, 6500 GL Nijmegen, The Netherlands
[18] Korea Astronomy and Space Science Institute, Daedeok-daero 776, Yuseong-gu, Daejeon 34055, Republic of Korea
[19] University of Science and Technology, Gajeong-ro 217, Yuseong-gu, Daejeon 34113, Republic of Korea
[20] Kavli Institute for Cosmological Physics, University of Chicago,
5640 South Ellis Avenue, Chicago, IL 60637, USA
[21] Department of Astronomy and Astrophysics, University of Chicago,
5640 South Ellis Avenue, Chicago, IL 60637, USA
[22] Department of Physics, University of Chicago,
5720 South Ellis Avenue, Chicago, IL 60637, USA
[23] Enrico Fermi Institute, University of Chicago, 5640 South Ellis Avenue, Chicago, IL 60637, USA
[24] Princeton Center for Theoretical Science, Jadwin Hall,
Princeton University, Princeton, NJ 08544, USA
[25] Data Science Institute, University of Arizona, 1230 N. Cherry Ave., Tucson, AZ 85721, USA
[26] Cornell Center for Astrophysics and Planetary Science, Cornell University, Ithaca, NY 14853, USA
[27] Anton Pannekoek Institute for Astronomy, University of Amsterdam,
Science Park 904, 1098 XH, Amsterdam, The Netherlands
[28] Shanghai Astronomical Observatory, Chinese Academy of Sciences,
80 Nandan Road, Shanghai 200030, People's Republic of China
[29] Key Laboratory of Radio Astronomy, Chinese Academy of Sciences, Nanjing 210008, People's Republic of China
[30] Department of Space, Earth and Environment, Chalmers University of Technology,
Onsala Space Observatory, SE-43992 Onsala, Sweden
[31] Mizusawa VLBI Observatory, National Astronomical Observatory of Japan,
2-12 Hoshigaoka, Mizusawa, Oshu, Iwate 023-0861, Japan
[32] Department of Astronomical Science, The Graduate University for Advanced
Studies (SOKENDAI), 2-21-1 Osawa, Mitaka, Tokyo 181-8588, Japan
[33] Dipartimento di Fisica "E. Pancini", Universitá di Napoli "Federico II",
Compl. Univ. di Monte S. Angelo, Edificio G, Via Cinthia, I-80126, Napoli, Italy
[34] Institut für Theoretische Physik, Goethe-Universität Frankfurt,
Max-von-Laue-Straße 1, D-60438 Frankfurt am Main, Germany
[35] INFN Sez. di Napoli, Compl. Univ. di Monte S. Angelo, Edificio G, Via Cinthia, I-80126, Napoli, Italy
[36] Department of Physics, University of Pretoria,
Lynnwood Road, Hatfield, Pretoria 0083, South Africa
[37] Centre for Radio Astronomy Techniques and Technologies,
Department of Physics and Electronics, Rhodes University, Grahamstown 6140, South Africa
[38] LESIA, Observatoire de Paris, Université PSL, CNRS, Sorbonne Université,
Université de Paris, 5 place Jules Janssen, 92195 Meudon, France
[39] JILA and Department of Astrophysical and Planetary Sciences,
University of Colorado, Boulder, CO 80309, USA
[40] Department of Physics, University of Illinois, 1110 West Green St, Urbana, IL 61801, USA
[41] Department of Astronomy, University of Illinois at Urbana-Champaign,
1002 West Green Street, Urbana, IL 61801, USA
[42] Leiden Observatory—Allegro, Leiden University,
P.O. Box 9513, 2300 RA Leiden, The Netherlands
[43] Key Laboratory for Research in Galaxies and Cosmology,
Chinese Academy of Sciences, Shanghai 200030, People's Republic of China
[44] NOVA Sub-mm Instrumentation Group, Kapteyn Astronomical Institute,
University of Groningen, Landleven 12, 9747 AD Groningen, The Netherlands
[45] Department of Astronomy, School of Physics, Peking University, Beijing 100871, People's Republic of China
[46] Kavli Institute for Astronomy and Astrophysics,
Peking University, Beijing 100871, People's Republic of China
[47] Department of Astronomy, Graduate School of Science,
The University of Tokyo, 7-3-1 Hongo, Bunkyo-ku, Tokyo 113-0033, Japan
[48] Instituto Nacional de Astrofísica, Óptica y Electrónica. Apartado Postal 51 y 216, 72000. Puebla Pue., México
[49] Max-Planck-Institut für Extraterrestrische Physik,
Giessenbachstr. 1, D-85748 Garching, Germany

[50] *Institute for Astrophysical Research, Boston University, 725 Commonwealth Ave., Boston, MA 02215, USA*
[51] *Astronomical Institute, St. Petersburg University, Universitetskij pr., 28, Petrodvorets,198504 St.Petersburg, Russia*
[52] *Perimeter Institute for Theoretical Physics, 31 Caroline Street North, Waterloo, ON, N2L 2Y5, Canada*
[53] *Department of Physics and Astronomy, University of Waterloo, 200 University Avenue West, Waterloo, ON, N2L 3G1, Canada*
[54] *Joint Institute for VLBI ERIC (JIVE), Oude Hoogeveensedijk 4, 7991 PD Dwingeloo, The Netherlands*
[55] *California Institute of Technology, 1200 East California Boulevard, Pasadena, CA 91125, USA*
[56] *Kogakuin University of Technology & Engineering, Academic Support Center, 2665-1 Nakano, Hachioji, Tokyo 192-0015, Japan*
[57] *Physics Department, National Sun Yat-Sen University, No. 70, Lien-Hai Rd, Kaosiung City 80424, Taiwan, R.O.C*
[58] *NSF's National Optical Infrared Astronomy Research Laboratory, 950 North Cherry Ave., Tucson, AZ 85719, USA*
[59] *Key Laboratory for Particle Astrophysics, Institute of High Energy Physics, Chinese Academy of Sciences, 19B Yuquan Road, Shijingshan District, Beijing, People's Republic of China*
[60] *School of Astronomy and Space Science, Nanjing University, Nanjing 210023, People's Republic of China*
[61] *Key Laboratory of Modern Astronomy and Astrophysics, Nanjing University, Nanjing 210023, People's Republic of China*
[62] *Max-Planck-Institut für Radioastronomie, Auf dem Hügel 69, D-53 121 Bonn, Germany*
[63] *Italian ALMA Regional Centre, INAF-Istituto di Radioastronomia, Via P. Gobetti 101, I-40129 Bologna, Italy*
[64] *Department of Physics, National Taiwan University, No.1, Sect.4, Roosevelt Rd., Taipei 10617, Taiwan, R.O.C*
[65] *Yunnan Observatories, Chinese Academy of Sciences, 650011 Kunming, Yunnan Province, People's Republic of China*
[66] *Center for Astronomical Mega-Science, Chinese Academy of Sciences, 20A Datun Road, Chaoyang District, Beijing, 100012, People's Republic of China*
[67] *Key Laboratory for the Structure and Evolution of Celestial Objects, Chinese Academy of Sciences, 650011 Kunming, People's Republic of China*
[68] *Gravitation Astroparticle Physics Amsterdam (GRAPPA) Institute, University of Amsterdam, Science Park 904, 1098 XH Amsterdam, The Netherlands*
[69] *Tsung-Dao Lee Institute, Shanghai Jiao Tong University, Shanghai, 200240, China*
[70] *Astronomy Department, Universidad de Concepción, Casilla 160-C, Concepción, Chile*
[71] *Department of Astronomy, University of Massachusetts, 01003, Amherst, MA, USA*
[72] *Canadian Institute for Theoretical Astrophysics, University of Toronto, 60 St. George Street, Toronto, ON M5S 3H8, Canada*
[73] *Dunlap Institute for Astronomy and Astrophysics, University of Toronto, 50 St. George Street, Toronto, ON M5S 3H4, Canada*
[74] *Canadian Institute for Advanced Research, 180 Dundas St West, Toronto, ON M5G 1Z8, Canada*
[75] *Radio Astronomy Laboratory, University of California, Berkeley, CA 94720, USA*
[76] *Department of Astrophysical Sciences, Peyton Hall, Princeton University, Princeton, NJ 08544, USA*
[77] *Center for Computational Astrophysics, Flatiron Institute, 162 Fifth Avenue, New York, NY 10010, USA*
[78] *CCS-2, Los Alamos National Laboratory, P.O. Box 1663, Los Alamos, NM 87545, USA*
[79] *Center for Theoretical Astrophysics, Los Alamos National Laboratory, Los Alamos, NM, 87545, USA*
[80] *Instituto de Radioastronomía Milimétrica, IRAM, Avenida Divina Pastora 7, Local 20, E-18012, Granada, Spain*
[81] *Consejo Nacional de Ciencia y Tecnología, Av. Insurgentes Sur 1582, 03940, Ciudad de México, México*
[82] *Hiroshima Astrophysical Science Center, Hiroshima University, 1-3-1 Kagamiyama, Higashi-Hiroshima, Hiroshima 739-8526, Japan*
[83] *Aalto University Department of Electronics and Nanoengineering, PL 15500, FI-00076 Aalto, Finland*
[84] *Aalto University Metsähovi Radio Observatory, Metsähovintie 114, FI-02540 Kylmälä, Finland*
[85] *Department of Astronomy, Yonsei University, Yonsei-ro 50, Seodaemun-gu, 03722 Seoul, Republic of Korea*
[86] *Netherlands Organisation for Scientific Research (NWO), Postbus 93138, 2509 AC Den Haag, The Netherlands*
[87] *Department of Physics and Astronomy, Seoul National University, Gwanak-gu, Seoul 08826, Republic of Korea*
[88] *Leiden Observatory, Leiden University, Postbus 2300, 9513 RA Leiden, The Netherlands*
[89] *Physics Department, Brandeis University, 415 South Street, Waltham, MA 02453, USA*
[90] *Jeremiah Horrocks Institute, University of Central Lancashire, Preston PR1 2HE, UK*
[91] *School of Physics, Huazhong University of Science and Technology, Wuhan, Hubei, 430074, People's Republic of China*

[92] *Mullard Space Science Laboratory, University College London, Holmbury St. Mary, Dorking, Surrey, RH5 6NT, UK*
[93] *School of Astronomy and Space Sciences, University of Chinese Academy of Sciences, No. 19A Yuquan Road, Beijing 100049, People's Republic of China*
[94] *Astronomy Department, University of Science and Technology of China, Hefei 230026, People's Republic of China*

The 2017 Event Horizon Telescope (EHT) observations of the central source in M87 have led to the first measurement of the size of a black-hole shadow. This observation offers a new and clean gravitational test of the black-hole metric in the strong-field regime. We show analytically that spacetimes that deviate from the Kerr metric but satisfy weak-field tests can lead to large deviations in the predicted black-hole shadows that are inconsistent with even the current EHT measurements. We use numerical calculations of regular, parametric, non-Kerr metrics to identify the common characteristic among these different parametrizations that control the predicted shadow size. We show that the shadow-size measurements place significant constraints on deviation parameters that control the second post-Newtonian and higher orders of each metric and are, therefore, inaccessible to weak-field tests. The new constraints are complementary to those imposed by observations of gravitational waves from stellar-mass sources.

Tests of general relativity have traditionally involved solar-system bodies [1] and neutron stars in binaries [2], for which precise measurements can be interpreted with minimal astrophysical complications. In recent years, observations at cosmological scales [3] and the detection of gravitational waves [4] have also resulted in an array of new gravitational tests.

The horizon-scale images of the black hole in the center of the M87 galaxy obtained by the EHT [5] offer the most recent addition to the set of observations that probe the strong-field regime of gravity. As an interferometer, the EHT measures the Fourier components of the brightness distribution of the source on the sky at a small number of distinct Fourier frequencies. The features of the underlying image are then reconstructed either using agnostic imaging algorithms or by directly fitting model images to the interferometric data. The central brightness depression seen in the M87 image has been interpreted as the shadow cast by this supermassive black hole on the emission from the surrounding plasma. The observability of the shadow of the black hole in M87 and the one the center of the Milky Way, Sgr A*, had been predicted earlier based on the properties of the radiatively inefficient accretion flows around these objects and their large mass-to-distance ratios [6].

The outline of a black-hole shadow is the locus of the photon trajectories on the screen of a distant observer that, when traced backwards, become tangent to the surfaces of spherical photon orbits hovering just above the black-hole horizons [7]. The Boyer-Lindquist radii of these spherical photon orbits lie in the range $(1-4)M$, depending on the black-hole spin and the orientation of the angular momentum of the orbit [8] (here M is the mass of the black hole and we have set $G = c = 1$, where G is the gravitational constant, and c is the speed of light). It is the fact that the outlines of black-hole shadows encode in them the strong-field properties of the spacetimes that led to the early suggestion that they can be used in performing strong-field gravitational tests [9–11].

Even though the radii of the photon orbits have a strong dependence on spin, a fortuitous cancellation of the effects of frame dragging and of the quadrupole structure in the Kerr metric causes the outline of the shadow, as observed at infinity, to have a size and a shape that depends very weakly on the spin of the black hole or the orientation of the observer [10]. This cancellation occurs because, due to the no-hair theorem, the magnitude of the quadrupole moment of the Kerr metric is not an independent quantity but is instead always equal to the square of the black-hole spin. For all possible values of spin and inclination, the size of the shadow is $\simeq 5M \pm 4\%$ and its shape is nearly circular to within $\sim 7\%$. For a black hole of known mass-to-distance ratio, the constancy of the shadow size allows for a null-hypothesis test of the Kerr metric [12]. At the same time, the nearly circular shape of the shadow offers the possibility of testing the gravitational no-hair theorem [10].

The first inference of the size of the black-hole shadow in M87 used as a proxy the measurement of the size of the bright ring of emission that surrounds the shadow and calibrated the difference in size via large suites of GRMHD simulations [5]. When this ring of emission is narrow, as is the case for the 2017 EHT image of M87, potential biases in the measurement are small. The inferred size of the M87 black-hole shadow was found to be consistent (to within $\sim 17\%$ at the 68-percentile level) with the predicted size based on the Kerr metric and the mass-to-distance ratio of the black hole derived using stellar dynamics [5, 13] (see, however, [14, 15] and [16]). The agreement between the measured and predicted shadow size does constitute a null-hypothesis test of the GR predictions: the data give us no reason to question the validity of the assumptions that went into this measurement, the Kerr metric being one of them. However, using this measurement to place quantitative constraints on any potential deviations from the Kerr metric is less straightforward for two reasons.

First, the Kerr metric is the unique black-hole so-

lution to a large number of modified gravity theories that are Lorentz symmetric and have field equations with constant coupling coefficients between the various gravitating fields [17, 18]. Only a limited number of black-hole solutions are known for theories with dynamical couplings [19] (e.g., dynamical Chern-Simons gravity and Einstein-dilaton-Gauss-Bonnet gravity [20]) or for Lorentz-violating theories [21]. Despite substantial progress in recent years, this line of work leads to limited theoretical guidance on the form and magnitude of potential deviations from the Kerr metric.

Second, if we instead use an empirical parametric framework to extend the Kerr metric, we would find that most naive parametric extensions lead to pathologies, such as non-Lorentzian signatures, singularities, and closed timelike loops, which render it impossible to calculate photon trajectories in the strong-field regime (see, e.g., [22]). In recent years, this problem has been addressed with the development of a number of parametric extensions of the Kerr metric that are free of pathologies [23–29]. Resolving the pathologies, however, comes at the cost of very large complexity. In principle, we can use the EHT measurement with any of these parametric extensions to place constraints on the specific parameters of the metric we used [30]. However, understanding the physical meaning of such constraints and comparing them with the constraints imposed when other parametric extensions are used are not readily feasible. In addition, the complexity of the various parametric extensions to the Kerr metric hinders the comparison of these gravitational tests with the results of other, e.g., weak-field and cosmological ones and, therefore, the effort to place complementary tests on the underlying gravity theory.

In this *Letter*, we use analytic arguments as well as numerical calculations of shadows to set new constraints on gravity using the 2017 EHT measurements, elucidate their physical meaning, and compare them with earlier weak-field tests. We find that the EHT measurements place constraints primarily on the $tt-$element of the black-hole spacetime (when the latter is expressed in areal coordinates and in covariant form). This is analogous to the fact that solar-system tests that involve gravitational lensing or Shapiro delay measurements constrain primarily one of the metric elements of the PPN framework [1]. However, we show that the constraints imposed by the EHT measurements are of (at least) the second post-Newtonian order and are, therefore, beyond the reach of weak-field experiments.

The size of the black-hole shadow both in the Kerr metric and in other parametric extensions depends very weakly on the black-hole spin [10, 31, 32]. For this reason, we start by exploring analytically the shadow size for a general static, spherically symmetric metric of the form

$$ds^2 = g_{tt}dt^2 + g_{rr}dr^2 + r^2 d\Omega \,. \tag{1}$$

Note that the choice of coordinates we use here is different from the isotropic coordinates of the PPN framework. We made this choice because, as we will show below, the radius of the photon orbit and the size of the shadow depend only on this element of the metric in these coordinates (unlike, e.g., Eq. [101] of Ref. [33], which is written in isotropic coordinates).

TABLE I. PPN expansions of various parametric extensions to the Kerr metric

Metric	$\bar{\beta}-\bar{\gamma}$ (1PN)	ζ (2PN)
Kerr	0	0
JP	0	α_{13}
MGBK	$-\gamma_{1,2}/2-\gamma_{4,2}\to 0$	$-\gamma_{1,2}-4\gamma_{4,2}\to\gamma_{1,2}$

Without loss of generality, we consider photon trajectories in the equatorial plane, i.e., set $\theta=\pi/2$. Following Ref. [34], we use two of the Killing vectors of the spacetime to write the components of the momentum of a photon traveling in this spacetime as

$$(k^t,k^r,k^\theta,k^\phi)=\left(\frac{E}{g_{tt}},\left[-\frac{E^2}{g_{tt}\,g_{rr}}-\frac{l^2}{g_{rr}r^2}\right]^{1/2},0,\frac{l}{r^2}\right)\,, \tag{2}$$

where E and l are the conserved energy and angular momentum of the photon and we have used the null condition $\underset{\sim}{k}\cdot\underset{\sim}{k}=0$ to calculate the radial component of the momentum.

The location of the circular photon orbit is the solution of the two conditions $k^r=0$ and $dk^r/dr=0$. Combining them, we write the radius $r_{\rm ph}$ of the photon orbit as the solution to the implicit equation

$$r_{\rm ph}=\sqrt{-g_{tt}}\left(\left.\frac{d\sqrt{-g_{tt}}}{dr}\right|_{r_{\rm ph}}\right)^{-1}\,. \tag{3}$$

The radius $r_{\rm sh}$ of the black-hole shadow as observed at infinity is the gravitationally lensed image of the circular photon orbit. This effect was calculated in Ref. [34] (Eq. [20]) and, when applied to the size of the photon orbit, leads to

$$r_{\rm sh}=\frac{r_{\rm ph}}{\sqrt{-g_{tt}(r_{\rm ph})}}\,. \tag{4}$$

As advertised earlier, both the radius of the photon orbit and the size of the black-hole shadow depend only on the tt element of the metric (1) written in areal coordinates and in covariant form.

In order to connect the strong-field constraints from black-hole shadows to the weak-field tests, we expand the tt element in powers of r^{-1} as

$$-g_{tt}=1-\frac{2}{r}+2\left(\frac{\bar{\beta}-\bar{\gamma}}{r^2}\right)-2\left(\frac{\zeta}{r^3}\right)+\mathcal{O}\left(r^{-4}\right)\,. \tag{5}$$

Hereafter, we set $G=c=M=1$, where G is the gravitational constant, c is the speed of light, and M is the

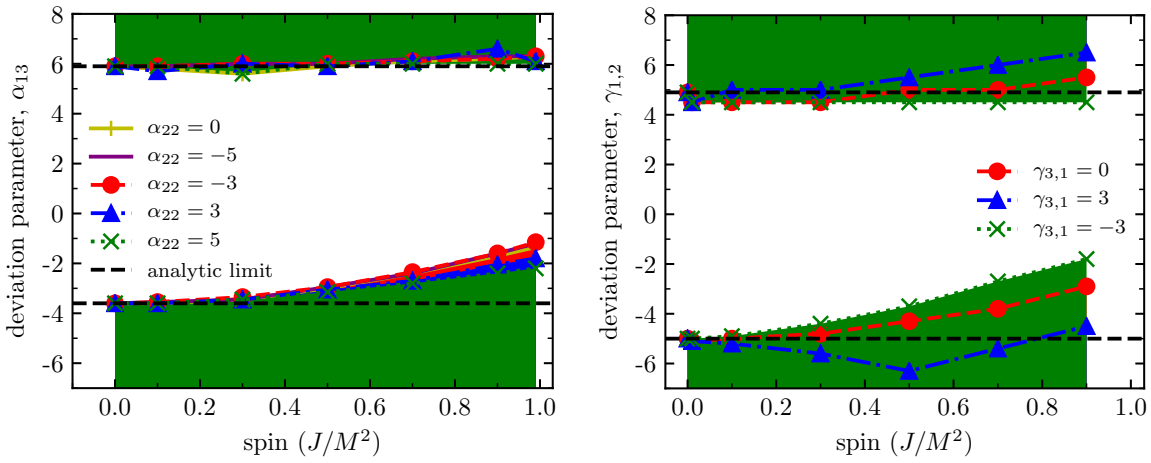

FIG. 1. Bound on the deviation parameters *(Left)* α_{13} of the JP metric and *(Right)* $\gamma_{1,2}$ for the MGBK metric, as a function of spin (J/M^2) and for different values of the other metric parameters, placed by the 2017 EHT observations of M87. The shaded areas show the excluded regions of the parameter space. The dashed line shows the analytic result obtained for zero spin. The EHT measurements place constraints predominantly on α_{13} (for JP) and $\gamma_{1,2}$ (for MGBK), which control the 2PN expansion of the corresponding metrics (see Table I).

black-hole mass. In this equation, we have employed the usual PPN parameters $\bar{\beta}$ and $\bar{\gamma}$ and added a 2PN term parametrized by the quantity ζ. Weak-field tests have placed strong constraints on the 1PN parameters to be equal to unity to within a few parts in 10^5 [1]. Even though modified gravity theories may not satisfy Birkhoff's theorem and, therefore, the values of the 1PN parameters may be different outside the Sun and outside a black hole, we make here the very conservative assumption that the solar-system limits are applicable to the external spacetimes of astrophysical black holes and set $\bar{\beta} - \bar{\gamma} \simeq 0$. If the tt element of the black-hole metric has indeed a vanishing 1PN term, as required by the weak-field tests, and terminates at the 2PN term, the radius of the circular photon orbit would be

$$r_{\rm ph} = 3 + \frac{5}{9}\zeta \tag{6}$$

and the size of the black-hole shadow would be

$$r_{\rm sh} = 3\sqrt{3}\left(1 + \frac{1}{9}\zeta\right) \ . \tag{7}$$

This is a quantitative demonstration of the fact that the size of the black-hole shadow probes the behavior of the spacetime at least at the 2PN order. Moreover, the size of the black-hole shadow depends linearly on the magnitude of the 2PN term.

To explore in detail the constraints imposed by the EHT results, we will consider, as concrete examples of regular, parametric extensions to the Kerr metric, the metrics developed in Refs. [22, 23] (hereafter the JP metric) and in Refs. [24, 35] (hereafter the MGBK metric). Table I shows the 1PN and 2PN parameters (see Eq. 1) for these metrics, when the spin parameter is set to zero and only leading orders of the parameters are considered. From the analytic argument above, we expect the shadow sizes to be determined primarily by the parameters that control the 2PN and higher-order terms for these metrics. Hereafter, we define the spin of a given metric as the dimensionless ratio J/M^2 of the lowest-order current moment, i.e, the angular momentum, to the square of the lowest-order mass moment, i.e., the Keplerian mass, of the spacetime.

The JP metric has four lowest-order parameters to describe possible deviations from Kerr [22]. The outlines of black-hole shadows for this metric have been calculated in Refs. [31, 32] and were shown to depend very weakly on the black-hole spin. Setting the spin to zero, we use Eq. (4) for the full metric to derive the shadow size as a function of the deviation parameters. We find that, in this limit, the shadow size depends entirely on one of the deviation parameters, α_{13}, which is also the one that controls the 2PN terms of the metric. The complete expression is very complicated to display here but a power-law expansion is

$$r_{\rm sh,JP} = 3\sqrt{3}\left[1 + \frac{1}{27}\alpha_{13} - \frac{1}{486}\alpha_{13}^2 + \mathcal{O}(\alpha_{13}^3)\right] \ . \tag{8}$$

Note that the coefficient of the deviation parameter α_{13} is different from what we would have expected from eq. (7) because the JP metric does not terminate at the 2PN order. Requiring that the shadow size is consistent to within 17% with the 2017 EHT measurement for M87 places a bound on the deviation parameter $-3.6 < \alpha_{13} < 5.9$. The left panel of Fig. 1 shows the corresponding limits on α_{13} obtained numerically from

the full JP metric, when the black-hole spin is taken into account and the second metric parameter that affects the shadow size for a spinning black hole, i.e., α_{22}, is varied. As evident here, the constraints on α_{13} change only mildly when effects that introduce deviations from spherical symmetry are included. Therefore, for the JP metric, the EHT measurement constrains predominantly the deviation parameter α_{13}, which controls the 2PN terms.

The MGBK metric has four lowest-order parameters to describe possible deviations from Kerr [35] without requiring the 1PN deviation to vanish (see Table I). The outlines of black-hole shadows have been calculated in Ref. [32] and their overall sizes were shown to depend primarily on the parameters $\gamma_{3,3}$, $\gamma_{1,2}$, and $\gamma_{4,2}$ (see Fig. 8 of [32]). In its original formulation, the parameter $\gamma_{3,3}$ describes frame dragging in a manner that remains finite even for nonspinning black holes (see Eq. [17] of [35]). Here, we scale this parameter with spin, i.e., write $\gamma'_{3,3} = \gamma_{3,3} a$ to remove the divergent behavior of the shadow size with $a \to 0$ found in Ref. [32]. We also set $\gamma_{4,2} = -\gamma_{1,2}/2$ for this metric to be consistent with Solar System tests at the 1PN order. In this case, the magnitude of potential 2PN deviations becomes equal to $\zeta_{\rm MGBK} = \gamma_{1,2}$.

With these redefinitions, the size of the shadow for the MGBK metric depends primarily on parameter $\gamma_{1,2}$ and only weakly on spin. As before, we calculate analytically the shadow size for this metric using Eq. (4) having set the spin equal to zero. We again display only an expansion of the size in the deviation parameter $\gamma_{1,2}$:

$$r_{\rm sh,MGBK} = 3\sqrt{3}\left[1 + \frac{1}{27}\gamma_{1,2} + \mathcal{O}(\gamma_{1,2}^3)\right] . \qquad (9)$$

Requiring that the shadow size is consistent to within 17% with the 2017 EHT measurement for M87 places a bound on the deviation parameter $-5.0 < \gamma_{1,2} < 4.9$. The right panel of Fig. 1 shows the corresponding constraints obtained numerically from the full solution, when the black-hole spin is taken into account and the other deviation parameters are varied. Again, the constraints on $\gamma_{1,2}$ change only mildly when effects that introduce deviations from spherical symmetry are included.

Even though the complex functional forms of the various elements in the two metrics we considered here are very different from each other, in both cases the predicted size of the black-hole shadow depends almost exclusively (and in a very similar manner) on the deviation parameter that controls the 2PN and higher-order terms for each metric. This conclusion remains the same when we use, e.g., the RZ metric [29], for which the deviations from Kerr are introduced by a sequence of parameters, with a_i controlling primarily the $i+1$ PN order. For this metric, $\zeta = -4\alpha_1$ and requiring that the predicted shadow size is consistent with the EHT measurements leads to the constraint $-1.2 < \alpha_1 < 1.3$. This supports our conclusion that an EHT measurement of the size of a black hole leads to metric tests that are inaccessible to weak-field tests.

In this Letter we have allowed for only one of the high-order PN parameters of the g_{tt} component of each metric to deviate from its Kerr value in order to show that significant constraints can be obtained even with the current EHT results. However, if more than one PN parameters of the same metric component are included, then the size measurement of the black-hole shadow will instead lead to a constraint on a linear combination of these parameters. Similar constraints will be possible in the very near future with EHT observations of the black hole in the center of the Milky Way, for which there is no ambiguity in the inferred mass. In that case, monitoring of individual stellar orbits has provided very precise measurements of its mass-to-distance ratio [36] leading to a prediction of $47-53$ μas for its shadow diameter, depending on the black-hole spin.

Observations of double neutron stars [2] and of coalescing black holes with LIGO/VIRGO [4] also probe the strong-field properties of their gravitational fields and lead to post-Newtonian constraints of similar magnitude as the ones we obtain here. The mass and curvature scale of the stellar-mass sources are eight orders of magnitude different from those of the M87 black hole, thereby probing a very different regime of gravitational parameters [5, 11]. It is this combination of gravitational tests across different scales that will provide complementary and comprehensive constraints on possible modifications of the fundamental gravitational theory.

The authors of the present paper thank the following organizations and programs: the Academy of Finland (projects 274477, 284495, 312496); the Advanced European Network of E-infrastructures for Astronomy with the SKA (AENEAS) project, supported by the European Commission Framework Programme Horizon 2020 Research and Innovation action under grant agreement 731016; the Alexander von Humboldt Stiftung; the Black Hole Initiative at Harvard University, through a grant (60477) from the John Templeton Foundation; the China Scholarship Council; Comisión Nacional de Investigación Científica y Tecnológica (CONICYT, Chile, via PIA ACT172033, Fondecyt projects 1171506 and 3190878, BASAL AFB-170002, ALMA-conicyt 31140007); Consejo Nacional de Ciencia y Tecnología (CONACYT, Mexico, projects 104497, 275201, 279006, 281692); the Delaney Family via the Delaney Family John A. Wheeler Chair at Perimeter Institute; Dirección General de Asuntos del Personal Académico—Universidad Nacional Autónoma de México (DGAPA—UNAM, project IN112417); the European Research Council Synergy Grant "BlackHoleCam: Imaging the Event Horizon of Black Holes" (grant 610058); the Generalitat Valenciana postdoctoral grant APOSTD/2018/177 and GenT Program (project CIDEGENT/2018/021); the

Gordon and Betty Moore Foundation (grants GBMF-3561, GBMF-5278); the Istituto Nazionale di Fisica Nucleare (INFN) sezione di Napoli, iniziative specifiche TEONGRAV; the International Max Planck Research School for Astronomy and Astrophysics at the Universities of Bonn and Cologne; the Jansky Fellowship program of the National Radio Astronomy Observatory (NRAO); the Japanese Government (Monbukagakusho: MEXT) Scholarship; the Japan Society for the Promotion of Science (JSPS) Grant-in-Aid for JSPS Research Fellowship (JP17J08829); the Key Research Program of Frontier Sciences, Chinese Academy of Sciences (CAS, grants QYZDJ-SSW-SLH057, QYZDJSSW-SYS008, ZDBS-LY-SLH011); the Leverhulme Trust Early Career Research Fellowship; the Max-Planck-Gesellschaft (MPG); the Max Planck Partner Group of the MPG and the CAS; the MEXT/JSPS KAKENHI (grants 18KK0090, JP18K13594, JP18K03656, JP18H03721, 18K03709, 18H01245, 25120007); the MIT International Science and Technology Initiatives (MISTI) Funds; the Ministry of Science and Technology (MOST) of Taiwan (105- 2112-M-001-025-MY3, 106-2112-M-001-011, 106-2119- M-001-027, 107-2119-M-001-017, 107-2119-M-001-020, and 107-2119-M-110-005); the National Aeronautics and Space Administration (NASA, Fermi Guest Investigator grant 80NSSC17K0649 and Hubble Fellowship grant HST-HF2-51431.001-A awarded by the Space Telescope Science Institute, which is operated by the Association of Universities for Research in Astronomy, Inc., for NASA, under contract NAS5-26555); the National Institute of Natural Sciences (NINS) of Japan; the National Key Research and Development Program of China (grant 2016YFA0400704, 2016YFA0400702); the National Science Foundation (NSF, grants AST-0096454, AST-0352953, AST-0521233, AST-0705062, AST- 0905844, AST-0922984, AST-1126433, AST-1140030, DGE-1144085, AST-1207704, AST-1207730, AST- 1207752, MRI-1228509, OPP-1248097, AST-1310896, AST-1312651, AST-1337663, AST-1440254, AST- 1555365, AST-1715061, AST-1615796, AST-1716327, OISE-1743747, AST-1816420); the Natural Science Foundation of China (grants 11573051, 11633006, 11650110427, 10625314, 11721303, 11725312, 11933007); the Natural Sciences and Engineering Research Council of Canada (NSERC, including a Discovery Grant and the NSERC Alexander Graham Bell Canada Graduate Scholarships-Doctoral Program); the National Youth Thousand Talents Program of China; the National Research Foundation of Korea (the Global PhD Fellowship Grant: grants NRF-2015H1A2A1033752, 2015-R1D1A1A01056807, the Korea Research Fellowship Program: NRF-2015H1D3A1066561); the Netherlands Organization for Scientific Research (NWO) VICI award (grant 639.043.513) and Spinoza Prize SPI 78-409; the New Scientific Frontiers with Precision Radio Interferometry Fellowship awarded by the South African Radio Astronomy Observatory (SARAO), which is a facility of the National Research Foundation (NRF), an agency of the Department of Science and Technology (DST) of South Africa; the Onsala Space Observatory (OSO) national infrastructure, for the provisioning of its facilities/observational support (OSO receives funding through the Swedish Research Council under grant 2017-00648) the Perimeter Institute for Theoretical Physics (research at Perimeter Institute is supported by the Government of Canada through the Department of Innovation, Science and Economic Development and by the Province of Ontario through the Ministry of Research, Innovation and Science); the Russian Science Foundation (grant 17-12-01029); the Spanish Ministerio de Economía y Competitividad (grants AYA2015-63939-C2-1-P, AYA2016-80889-P, PID2019-108995GB-C21); the State Agency for Research of the Spanish MCIU through the "Center of Excellence Severo Ochoa" award for the Instituto de Astrofísica de Andalucía (SEV-2017- 0709); the Toray Science Foundation; the Consejería de Economía, Conocimiento, Empresas y Universidad of the Junta de Andalucía (grant P18-FR-1769), the Consejo Superior de Investigaciones Científicas (grant 2019AEP112); the US Department of Energy (USDOE) through the Los Alamos National Laboratory (operated by Triad National Security, LLC, for the National Nuclear Security Administration of the USDOE (Contract 89233218CNA000001)); the Italian Ministero dell'Istruzione Università e Ricerca through the grant Progetti Premiali 2012-iALMA (CUP C52I13000140001); the European Union's Horizon 2020 research and innovation programme under grant agreement No 730562 RadioNet; ALMA North America Development Fund; the Academia Sinica; Chandra TM6-17006X; the GenT Program (Generalitat Valenciana) Project CIDEGENT/2018/021. This work used the Extreme Science and Engineering Discovery Environment (XSEDE), supported by NSF grant ACI-1548562, and CyVerse, supported by NSF grants DBI-0735191, DBI-1265383, and DBI-1743442. We thank the staff at the participating observatories, correlation centers, and institutions for their enthusiastic support. ALMA is a partnership of the European Southern Observatory (ESO; Europe, representing its member states), NSF, and National Institutes of Natural Sciences of Japan, together with National Research Council (Canada), Ministry of Science and Technology (MOST; Taiwan), Academia Sinica Institute of Astronomy and Astrophysics (ASIAA; Taiwan), and Korea Astronomy and Space Science Institute (KASI; Republic of Korea), in cooperation with the Republic of Chile. The Joint ALMA Observatory is operated by ESO, Associated Universities, Inc. (AUI)/NRAO, and the National Astronomical Observatory of Japan (NAOJ). The NRAO is a facility of the NSF operated under cooperative agreement by AUI. APEX is a collaboration between the Max-Planck-Institut fur Ra-

dioastronomie (Germany), ESO, and the Onsala Space Observatory (Sweden). The SMA is a joint project between the SAO and ASIAA and is funded by the Smithsonian Institution and the Academia Sinica. The JCMT is operated by the East Asian Observatory on behalf of the NAOJ, ASIAA, and KASI, as well as the Ministry of Finance of China, Chinese Academy of Sciences, and the National Key R&D Program (No. 2017YFA0402700) of China. Additional funding support for the JCMT is provided by the Science and Technologies Facility Council (UK) and participating universities in the UK and Canada. The LMT is a project operated by the Instituto Nacional de Astrofisica, Optica, y Electronica (Mexico) and the University of Massachusetts at Amherst (USA). The IRAM 30-m telescope on Pico Veleta, Spain is operated by IRAM and supported by CNRS (Centre National de la Recherche Scientifique, France), MPG (Max-Planck- Gesellschaft, Germany) and IGN (Instituto Geográfico Nacional, Spain). The SMT is operated by the Arizona Radio Observatory, a part of the Steward Observatory of the University of Arizona, with financial support of operations from the State of Arizona and financial support for instrumentation development from the NSF. The SPT is supported by the National Science Foundation through grant PLR- 1248097. Partial support is also provided by the NSF Physics Frontier Center grant PHY-1125897 to the Kavli Institute of Cosmological Physics at the University of Chicago, the Kavli Foundation and the Gordon and Betty Moore Foundation grant GBMF 947. The SPT hydrogen maser was provided on loan from the GLT, courtesy of ASIAA. The EHTC has received generous donations of FPGA chips from Xilinx Inc., under the Xilinx University Program. The EHTC has benefited from technology shared under open-source license by the Collaboration for Astronomy Signal Processing and Electronics Research (CASPER). The EHT project is grateful to T4Science and Microsemi for their assistance with Hydrogen Masers. This research has made use of NASA's Astrophysics Data System. We gratefully acknowledge the support provided by the extended staff of the ALMA, both from the inception of the ALMA Phasing Project through the observational campaigns of 2017 and 2018. We would like to thank A. Deller and W. Brisken for EHT-specific support with the use of DiFX. We acknowledge the significance that Maunakea, where the SMA and JCMT EHT stations are located, has for the indigenous Hawaiian people.

[1] C. M. Will, Living Reviews in Relativity **17**, 4 (2014).
[2] N. Wex, arXiv e-prints , arXiv:1402.5594 (2014).
[3] P. G. Ferreira, Ann. Rev. Astron. Astrophys. **57**, 335 (2019).
[4] B. P. Abbott, et al, LIGO Scientific, and Virgo Collaborations, Phys. Rev. Lett. **116**, 221101 (2016); Phys. Rev. D **100**, 104036 (2019); M. Isi, M. Giesler, W. M. Farr, M. A. Scheel, and S. A. Teukolsky, Phys. Rev. Lett. **123**, 111102 (2019).
[5] Event Horizon Telescope Collaboration, Astrophys. J. Lett. **875**, L1 (2019); Astrophys. J. Lett. **875**, L2 (2019); Astrophys. J. Lett. **875**, L3 (2019); Astrophys. J. Lett. **875**, L4 (2019); Astrophys. J. Lett. **875**, L5 (2019); Astrophys. J. Lett. **875**, L6 (2019).
[6] H. Falcke, F. Melia, and E. Agol, Astrophys. J. Lett. **528**, L13 (2000); F. Özel, D. Psaltis, and R. Narayan, Astrophys. J. **541**, 234 (2000); F. Özel and T. Di Matteo, Astrophys. J. **548**, 213 (2001).
[7] J. M. Bardeen, in *Black Holes (Les Astres Occlus)*, edited by C. Dewitt and B. S. Dewitt (1973) pp. 215–239; S. Chandrasekhar, *The mathematical theory of black holes* (1983); E. Teo, GRG **35**, 1909 (2003); R. Takahashi, Astrophys. J. **611**, 996 (2004).
[8] J. M. Bardeen, W. H. Press, and S. A. Teukolsky, Astrophys. J. **178**, 347 (1972).
[9] C. Bambi and K. Freese, Phys. Rev. D **79**, 043002 (2009).
[10] T. Johannsen and D. Psaltis, Astrophys. J. **718**, 446 (2010).
[11] D. Psaltis, GRG **51**, 137 (2019); P. V. P. Cunha and C. A. R. Herdeiro, GRG **50**, 42 (2018); T. Baker, D. Psaltis, and C. Skordis, Astrophys. J. **802**, 63 (2015).
[12] D. Psaltis, F. Özel, C.-K. Chan, and D. P. Marrone, Astrophys. J. **814**, 115 (2015).
[13] K. Gebhardt, J. Adams, D. Richstone, T. R. Lauer, S. M. Faber, K. Gültekin, J. Murphy, and S. Tremaine, Astrophys. J. **729**, 119 (2011).
[14] J. L. Walsh, A. J. Barth, L. C. Ho, and M. Sarzi, Astrophys. J. **770**, 86 (2013).
[15] J. Kormendy and L. C. Ho, Ann. Rev. Astron. Astrophys. **51**, 511 (2013).
[16] A second technique of measuring the mass of M87 based on gas dynamics results in a mass that is smaller by a factor of 2. However, the accuracy of this technique has been questioned as it often leads to underestimated black-hole masses [15]. Moreover, choosing this mass instead would lead us to the conclusion that the metric of the M87 black hole deviates substantially from Kerr. We consider this to be a rather unlikely possibility and, therefore, give a negligible prior to the mass measurement from gas dynamics.
[17] D. Psaltis, D. Perrodin, K. R. Dienes, and I. Mocioiu, Phys. Rev. Lett. **100**, 091101 (2008).
[18] T. P. Sotiriou and V. Faraoni, Phys. Rev. Lett. **108**, 081103 (2012).
[19] E. Berti and et al., CQG **32**, 243001 (2015).
[20] N. Yunes and L. C. Stein, Phys. Rev. D **83**, 104002 (2011); K. Yagi, N. Yunes, and T. Tanaka, Phys. Rev. D **86**, 044037 (2012); D. Ayzenberg and N. Yunes, Phys. Rev. D **90**, 044066 (2014); R. McNees, L. C. Stein, and N. Yunes, Classical and Quantum Gravity **33**, 235013 (2016); H. O. Silva, J. Sakstein, L. Gualtieri, T. P. Sotiriou, and E. Berti, Phys. Rev. Lett. **120**, 131104 (2018); D. D. Doneva and S. S. Yazadjiev, Phys. Rev. Lett. **120**, 131103 (2018).
[21] E. Barausse, T. Jacobson, and T. P. Sotiriou, Phys. Rev. D **83**, 124043 (2011); E. Barausse and T. P. Sotiriou, Classical and Quantum Gravity **30**, 244010 (2013); E. Barausse, T. P. Sotiriou, and I. Vega, Phys. Rev. D **93**, 044044 (2016); O. Ramos and E. Barausse,

Phys. Rev. D **99**, 024034 (2019).
[22] T. Johannsen, Phys. Rev. D **87**, 124017 (2013).
[23] T. Johannsen and D. Psaltis, Phys. Rev. D **83**, 124015 (2011).
[24] S. Vigeland, N. Yunes, and L. C. Stein, Phys. Rev. D **83**, 104027 (2011).
[25] T. Johannsen, Phys. Rev. D **88**, 044002 (2013).
[26] V. Cardoso, P. Pani, and J. Rico, Phys. Rev. D **89**, 064007 (2014).
[27] L. Rezzolla and A. Zhidenko, Phys. Rev. D **90**, 084009 (2014).
[28] V. Cardoso and L. Queimada, GRG **47**, 150 (2015).
[29] R. Konoplya, L. Rezzolla, and A. Zhidenko, Phys. Rev. D **93**, 064015 (2016).
[30] T. Johannsen, A. E. Broderick, P. M. Plewa, S. Chatzopoulos, S. S. Doeleman, F. Eisenhauer, V. L. Fish, R. Genzel, O. Gerhard, and M. D. Johnson, Phys. Rev. Lett. **116**, 031101 (2016).
[31] T. Johannsen, Astrophys. J. **777**, 170 (2013).
[32] L. Medeiros, D. Psaltis, and F. Özel, Astrophys. J. **896**, 7 (2020), arXiv:1907.12575 [astro-ph.HE].
[33] A. Sullivan, N. Yunes, and T. P. Sotiriou, Phys. Rev. D **101**, 044024 (2020).
[34] D. Psaltis, Phys. Rev. D **77**, 064006 (2008).
[35] J. Gair and N. Yunes, Phys. Rev. D **84**, 064016 (2011).
[36] Gravity Collaboration, Phys. Rev. Lett. **122**, 101102 (2019); Astron. Astrophys. **636**, L5 (2020); T. Do and et al., Science **365**, 664 (2019).